Check for updates

Influence of different alumina phases on the catalytic properties of palladium-alumina catalysts for selective hydrogenation of acetylene to ethylene

Kishore Ravindran[1,2] · G. Madhu[1] · V. R. Renjith[1] · Sreekala Rugmini[2]

Abstract

Selective hydrogenation of acetylene was studied using palladium catalysts supported on different transition alumina spheres. The alumina supports were prepared by calcining pseudo boehmite alumina sphere at different calcination temperatures; the ρ-Al_2O_3 used was flash calcined alumina. The alumina supports were characterized using different techniques like XRD, surface area, pore volume and acidity. The Pd/Al_2O_3 catalyst were prepared, palladium penetration depth was measured using microscopic imaging and the catalyst reducibility were studied by Temperature Programmed Reduction (TPR). The microscopic imaging using TEM were done to study the palladium particle size and nature of particle clusters on the support surface. The catalyst performance evaluation was done in a fixed bed reactor with 1% acetylene in nitrogen feed and studied the impact of support properties on the catalytic activity. The catalyst prepared on γ-Al_2O_3 support showed the highest conversion and lowest selectivity, whereas the catalyst on α-Al_2O_3 support has the lower conversion and highest selectivity. Thermogravimetric analysis coupled with mass spectroscopy analysis were done for the spent catalyst to understand the possibilities of heavy component deposition of the catalyst. The catalyst prepared on α-Al_2O_3 support had the lowest hydrocarbon deposit on the surface whereas the γ and δ alumina showed the highest hydrocarbon deposits on the catalyst surface.

Keywords Alumina phases · Pd/Al_2O_3 · Selective hydrogenation · Acetylene · Catalyst activity · Catalyst deactivation

---

✉ Kishore Ravindran
kishoreravindran999@gmail.com

[1] School of Engineering, Cochin University of Science and Technology, Kochi, India

[2] Sud-Chemie India (P) Limited, Edayar, Kochi, India

Introduction

Ethylene is one of the major chemicals used in the petrochemical industry. The majority of the ethylene is produced from steam cracking of naphtha like feedstocks. Ethylene from the steam cracker typically contains 0.1−1% acetylene. Acetylene impurities are typically removed by selective hydrogenation and by using adsorption technique. Selective hydrogenation is the most commonly used method [1]. Acetylene removal is important as it act as poison for the polyethylene catalyst. Selective hydrogenation for acetylene can be done in two-configurations: front-end hydrogenation and tail end hydrogenation. The tail end hydrogenation is the more common configuration due to its better process controllability. Pd/ Al_2O_3 first generation commercial catalysts were introduced in early 1960s after twenty years. The first bi metallic catalyst, palladium and silver on alumina was introduced after almost twenty years, which is still used successfully in the industry. The Pd–Ag alloy catalyst had good selectivity and the selectivity was improved by reducing the quantity of hydrogen adsorbed on the surface. The properties of the bi metallic catalyst depend on the preparation method, the support alumina, the impregnation sequence and other processing steps [2]. The alumina can be prepared in different phases, γ, δ, ρ, α. The different alumina phases have different properties and different stability. Palladium catalyst on different alumina phases were made and the properties of the catalyst was studied. Different alumina phases impart different characteristics to the catalyst and they influence the reaction yield, selectivity, the green oil formation etc. For the selective hydrogenation of acetylene, low surface area alumina supports are mostly used with the palladium content typically from 100–1000 ppm. Egg shell type catalysts are often used to avoid the mass transfer resistances in the catalyst bed [3]. In this paper, the impact of support properties on the catalyst performance and coke formation were studied.

Experimental

Preparation and characterisation of support and catalysts

Spheres of γ-Al_2O_3 and ρ-Al_2O_3 received from Sud-Chemie India (P) Ltd were used for the present study. γ-Al_2O_3 spheres were calcined at 900 °C and 1300 °C for 6 h to obtain δ-Al_2O_3 and α-Al_2O_3 spheres [4, 5]. The Al_2O_3 spheres were characterized using XRD (Bruker D2Phaser), surface area, pore volume and pore size (BET method—Micromeritics Tristar) and acidity measurements (ammonia TPD—Micromeritics Autochem II). The XRD scan was done at 2θ value ranging from 0 to 60. The results were evaluated using EVA software. The standard PDF files in repository were compared to identify the phases in each material using the Scan function [6–10]. For ammonia TPD measurements, 5% ammonia in helium was used as the analysis gas. The adsorption of ammonia on the alumina supports

was done at 40 °C and the gas flow continued until there is no further adsorption of ammonia was observed. Purged with helium to drive out the gas from pores and the sample was heated in helium gas at a ramp rate of 10 °C/ min. The ammonia desorbed was measured using a TCD detector and quantified the total desorbed quantity of ammonia [11].

The catalyst preparation on different alumina supports were done using wet impregnation method [12, 13]. Palladium source used for the catalyst preparation was palladium nitrate solution purchased from Sigma Aldrich. The catalyst was dried at 80 °C and further calcined at 400 °C. [14–16]. The active metal loading ranged from 190 to 200 ppm on the catalyst as analyzed by ICP. Temperature programmed reduction (TPR) of the catalysts was done using Micrometrics Autochem II equipment using 5% hydrogen in nitrogen as the reducing gas. The TCD signals were recorded from 40 °C to 600 °C. The plot gives the reduction temperatures of each catalyst sample [17, 18]. Palladium metal penetration depth measurement was done using Olympus microscope and software. Different alumina supports have different pore size distributions and different pore structure; hence the penetration depth also varies. The catalyst was sliced into half using a special tools and the image of the palladium metal penetration was taken [19]. TEM analysis of the catalyst samples were done using HR TEM Joel/JEM 2100 microscope to understand about the Pd particle in the catalysts.

Catalyst performance evaluation

The performance evaluation was done in a fixed bed reactor with dimension 25 mm ID and 1000 mm length. The thermocouple was adjusted to measure the catalyst bed temperature. The reactor tube is made of SS 316 L. The gas flow through the reactor controlled using mass flow controllers and the pressure regulation of the reactor done using backpressure regulating valve [20].

The catalyst (10 cm^3) was reduced with 5% hydrogen balance nitrogen at 5 bar pressure and 350 °C for 4 h. After catalyst reduction the reactor was cooled in nitrogen stream to 40 °C. The process gas containing 1% acetylene in nitrogen was passed through the reactor keeping the pressure at 5 bar g. The hydrogen to acetylene ratio is maintained 1.2 during the experiment. The reaction was done at different temperatures 60 °C, 70 °C, 80 °C and 90 °C at a GHSV of 3000 h^{-1}. At each temperature, the conditions were kept constant and the reaction was allowed to stabilize for the initial 1 h and reactor outlet gas was collected at an interval for 30 min. The reaction temperature was changed after collecting 3 samples from each temperature. [21, 22].

$$\text{Acetylene conversion} = \frac{C_2H_2 \ (in) - C_2H_2 \ (out)}{C_2H_2 \ (in)} \times 100 \qquad (1)$$

$$\text{Ethylene selectivity} = \frac{C_2H_4 \ (out)}{C_2H_2 \ (in) - C_2H_2 \ (out)} \times 100 \qquad (2)$$
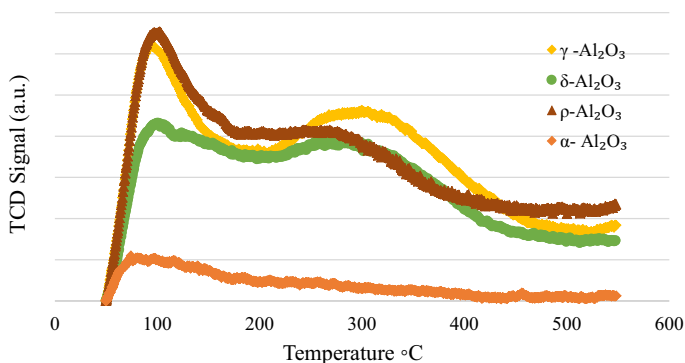
Fig. 1 Ammonia TPD plots of the support alumina. TPD done with Autochem II, in 5% ammonia in helium gas, with a heating ramp of 10 °C/ min

Table 1 Ammonia desorbed from different catalysts during ammonia TPD experiments

Sample	Desorption temperatures (°C)	Total quantity of NH_3 desorbed (µmol/g)
γ-Al_2O_3	94, 313	83.5
δ-Al_2O_3	102, 309	43.8
ρ-Al_2O_3	100, 277	11.5
α-Al_2O_3	87	2.3

$$Ethylene\ yield = Conversion \times Ethylene\ selectivity \qquad (3)$$

The outlet gas analysis was done using an Agilent GC 7890B with CP Al_2O_3 column.

The spent catalyst from the reaction were collected and thermogravimetric analysis (TA Instruments SDT Q 600) along with mass spectroscopy (MKS-Cirrus 2) analysis was done to study the coke/green oil formation in each catalyst. The analysis was performed in air from 25 to 1000 °C at a ramp rate of 10 °C/ min.

Results and discussion

Support characterization

The XRD of the samples were done and were compared with the standard files in the data bank to identify the phases. The crystallinity was very high in α Al_2O_3 support whereas γ-, δ- and ρ-Al_2O_3 show amorphous XRD pattern as expected. [23, 24]. The XRD comparison of different Al_2O_3 phases is provided in the supplementary data. Acidity measurement of the supports was performed in Micrometrics Autochem-II with ammonia temperature programmed desorption. The ammonia desorption with

Table 2 Physical characteristics of the support alumina

Sample ID	Surface area from BET analysis, m^2/g	Nitrogen pore volume, cm^3/g	Mean pore diameter, Å
γ-Al_2O_3	235	0.65	79.6
δ-Al_2O_3	131	0.55	134.2
ρ-Al_2O_3	270	0.40	53.5
α-Al_2O_3	10.5	0.04	–

Table 3 Catalyst physicochemical properties

Catalyst	Pd/γ-Al_2O_3	Pd/δ-Al_2O_3	Pd/ρ-Al_2O_3	Pd/α-Al_2O_3
Pd content, ppm	200	198	196	196
Surface area, m^2/g	235	131	270	10.2
Nitrogen PV, cm^3/g	0.62	0.50	0.35	0.028

the temperature shows the presence of weak and strong acid sites and the intensity varies in different phases of alumina (Fig. 1, Table 1).

The δ- and ρ-Al_2O_3 have relatively lower acidic sites compared to γ-Al_2O_3. The γ, δ- and ρ-Al_2O_3 has weak, medium and strong acid sites, the TPD peaks at temperatures above 200 °C indicates the presence medium and strong acid sites. In α-Al_2O_3, only very weak acid sites are present and the lower acidic sites help in lowering the alkylation reaction on alumina surface and consequently the polymerization and green oil formation [25, 26].

Different phases of Al_2O_3 exhibit different pore characteristics and SA (Table 2). The α-Al_2O_3 support has the lowest surface area and the lowest micro pore volume. The support mostly has macropores [27]. The γ-Al_2O_3 has the highest surface area and the highest nitrogen pore volume, indicating mostly micro and mesopores. The δ-Al_2O_3 also has lower nitrogen pore volume than γ-Al_2O_3 and lower surface area. The ρ-Al_2O_3 is entirely different type of alumina prepared by flash calcination and it has good surface area and relatively moderate pore volume [28].

Catalyst characterization

The catalyst properties like the metal content, surface area and pore volume are given in Table 3. No difference in surface area and pore volume was noticed for alumina before and after palladium impregnation. This indicates that the support is stable in palladium nitrate solution.

Temperature programmed reduction

The temperature-programmed reduction was performed using Micrometrics Autochem II instrument. The reductions were done using 5% hydrogen balance nitrogen

gas with a temperature ramp of 2 °C/min and the resulting curve with the peaks were plotted.

The negative dip in the TPR plot was due to the reduction of the bulk PdO forming palladium β hydride, which forms at a low temperature around 20 to 25 °C. This palladium β-hydride decomposes at a higher temperature and shows a negative peak while decomposing. The position of the negative peak depends on the type of the hydride formation, which depends on the size of the Palladium molecule and the dispersion of the palladium on the alumina support. Larger sized PdO particles have the palladium hydride decomposition at lower temperature and the smaller size PdO particles have the Palladium hydride decomposition at higher temperature. The highly dispersed palladium molecule has high intensity decomposition peak and at a higher temperature. The α-Al₂O₃ support has the lowest surface area and hence lower Pd dispersion, the Pd particles will be the largest in this catalyst. Larger Pd species forms hydrides easily and these hydrides decomposes at temperatures below 25 °C. The TPR profile of Pd /γ—Al₂O₃, Pd/ δ-Al₂O₃, Pd/ρ-Al₂O₃ shows negative dip in the TPR at peaks at 62 °C, 63 °C and 94 °C attributed to the decomposition of palladium hydride. The high temperatures peaks in the TPR at 228 °C, 248 °C, 306 °C and 400 °C will be due to the reduction of smaller PdO particles and hydrogen spill over on the alumina surface hydroxyl groups [29–31] (Fig. 2).
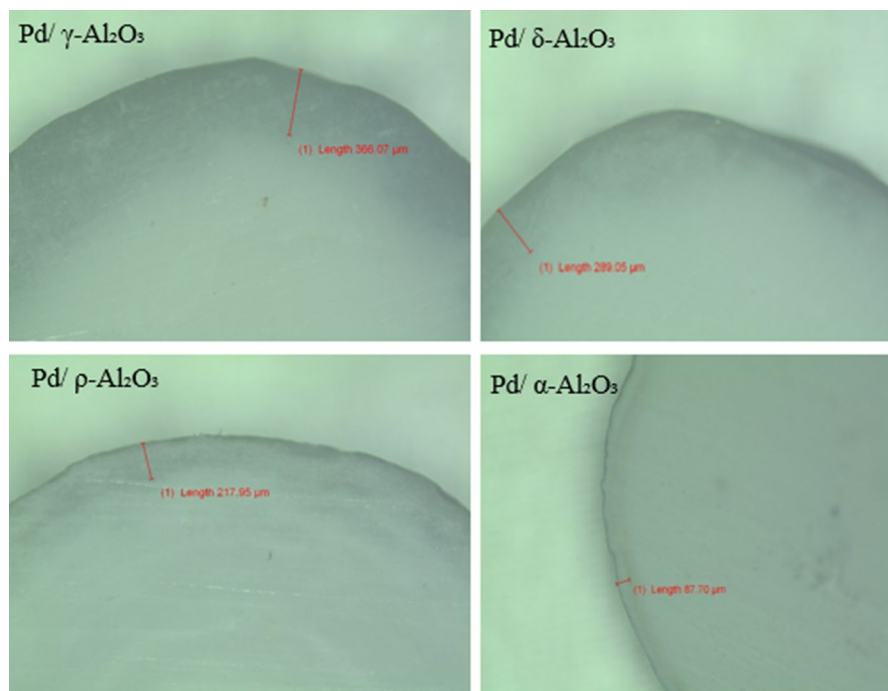
Palladium metal penetration depth measurement

Palladium metal penetration depth measurement was done using Olympus microscope and software. Different alumina support has different pore size distribution and different pore structure hence the penetration depth varies too. The catalyst was sliced into half using a special tools and the image of the palladium metal penetration was taken. Palladium penetration depth was measured for twenty sphere from each catalyst sample. The microscopy measurement pictures are displayed in Fig. 3.

The active metal penetration depth is highest for the γ-Al₂O₃, hence the active metal will be highly dispersed, and the metal penetration depth was lowest for α-Al₂O₃. Pd/α-Al₂O₃ catalyst has the thinnest active metal shell. Table 4 gives a
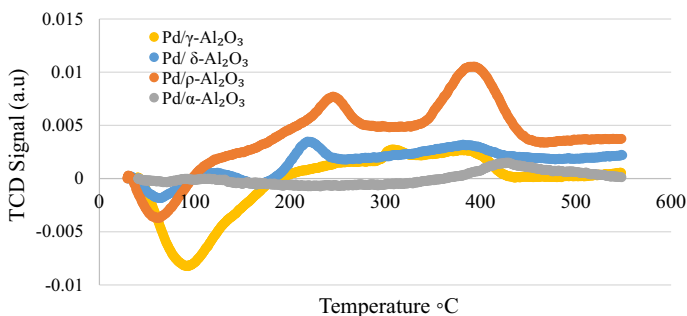
Fig. 2 TPR Plots of Pd/ Al₂O₃ catalysts. TPR done using Micromeritics Autochem-II with 5% hydrogen balance nitrogen mixture in a temperature range of 40 to 600 °C and with heating ramp rate of 2 °C/min

Fig. 3 Palladium penetration depth in the catalysts, measured using Olympus microscope after slicing the catalyst into half

**Table 4** Palladium metal penetration depth measurement results obtained from the microscopic analysis

Catalyst	Minimum (µm)	Average (µm)	Maximum (µm)
Pd/ γ-Al$_2$O$_3$	199.5	392.2	678.4
Pd/ δ-Al$_2$O$_3$	127.0	244.0	530.7
Pd/ ρ-Al$_2$O$_3$	126.3	222.5	392.0
Pd/ α-Al$_2$O$_3$	46.5	71.5	103.7

comparison of the penetration depth in the catalysts prepared with different supports (Fig. 3).

The selective hydrogenation reaction is a fast reaction and higher dispersion could make the catalyst more active and more prone to over hydrogenation [32, 33]. Hence better selectivity to ethylene can be expected for the catalyst with a typical egg-shell type palladium distribution.

TEM analysis of the catalysts

High-resolution transmission electron microscopy image were taken for the catalyst sample using Joel/JEM 2100 microscope. The images were taken at different resolutions and the particle size were analyzed (Fig. 4).
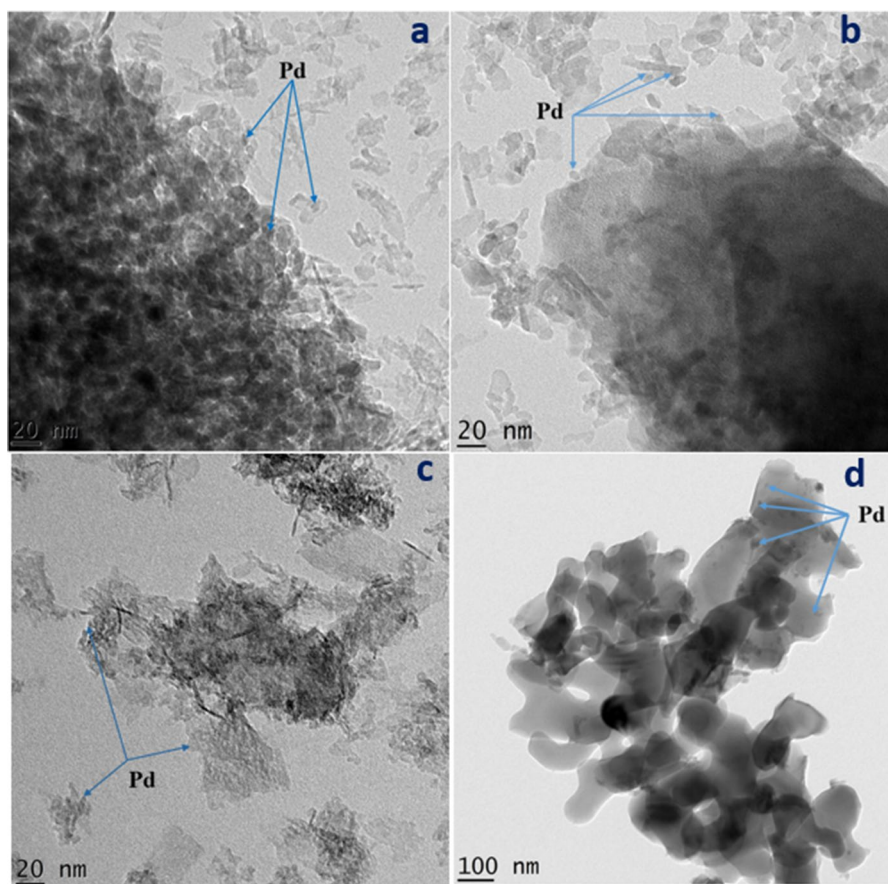
Fig. 4 HR TEM image of the catalysts taken using Joel/JEM2001 instrument **a** Pd/γ-Al$_2$O$_3$, **b** Pd/δ-Al$_2$O$_3$, **c** Pd/ρ-Al$_2$O$_3$, **d** Pd/α-Al$_2$O$_3$

HR TEM analysis reveals Pd particles on the Pd/α-Al$_2$O$_3$ has larger size compared to other catalysts. The Pd particles on the Pd/γ-Al$_2$O$_3$ and Pd/ρ-Al$_2$O$_3$ catalyst are relatively smaller and most of the particles are below 5 nm in size.

The palladium particle size distribution on catalysts were analyzed using the J-image software (Fig. 5). Particle size distributions were done by analyzing 20 particles in each catalysts and were plotted in a bar chart. The average Pd particle size were 4.7, 8.9, 4.3 and 10 nm on Pd/γ-Al$_2$O$_3$, Pd/δ-Al$_2$O$_3$, Pd/ρ-Al$_2$O$_3$ and Pd/α-Al$_2$O$_3$.

Catalyst performance evaluation

All the catalysts were tested for the selective hydrogenation of acetylene. The catalyst (10 cm^3) was loaded in the reactor and was reduced using 5% hydrogen in nitrogen at 370 °C and 5 bar gauge pressure for 3 h. The catalyst performance was
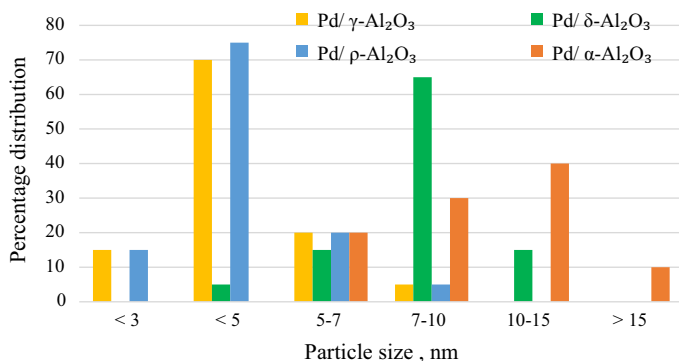
Fig. 5 Palladium particle size distribution from TEM image analysis analyzed over 20 particles

evaluated at different temperatures 60–90 °C at a GHSV 3000 h^{-1} and an operating pressure of 5 bar gauge (Fig. 6).

Catalyst Pd/γ-Al$_2$O$_3$ showed very high acetylene conversion and low ethylene selectivity at all temperatures. Ethylene selectivity of these catalysts was calculated using the formula and it was found that the catalyst Pd/α-Al$_2$O$_3$ has the highest selectivity and Pd/γ-Al$_2$O$_3$ has the lowest selectivity (Table 5). The selectivity of all the catalysts reduces drastically with increase in the operating temperature. The increased temperature favors ethane formation on the catalysts. Catalyst Pd/ρ-Al$_2$O$_3$ support has a different behavior compared to the others. The catalyst Pd/ρ-Al$_2$O$_3$ exhibits improvement in selectivity as the temperature was increased. Reaction temperatures were not increased beyond 90 °C and hence a separate study has to be
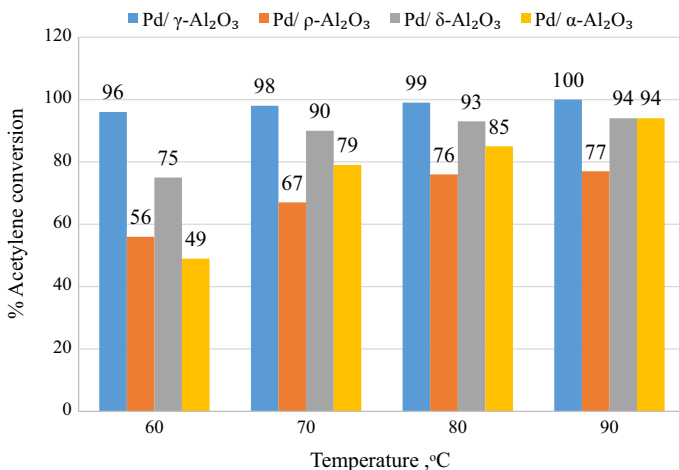
Fig. 6 Conversion of acetylene on different catalysts. Feed − 1% acetylene in nitrogen feed and hydrogen, hydrogen to acetylene molar ratio 1.2: 1, 10 cm^3 catalyst used, GHSV 3000 h^{-1}, 5 bar gauge pressure and operating temperature ranging from 60 °C to 90 °C

Table 5 Conversion, ethylene selectivity and ethylene yield data for different catalysts

Catalyst	Temperature °C	% Acetylene conversion	% Ethylene selectivity	%Ethylene yield
Pd/γ-Al$_2$O$_3$	60	96	29	27.8
	70	98	21	20.6
	80	99	13	12.9
	90	100	2.3	2.3
Pd/δ-Al$_2$O$_3$	60	75	47	35.3
	70	90	37	33.3
	80	93	38	35.3
	90	94	36	33.8
Pd/ρ-Al$_2$O$_3$	60	75	47	35.3
	70	90	37	33.3
	80	93	38	35.3
	90	94	36	33.8
Pd/α-Al$_2$O$_3$	60	49	70	34.3
	70	79	54	42.7
	80	85	48	40.8
	90	94	44	41.4

done to understand the behavior at high temperatures. The selectivity of the catalyst Pd/α-Al$_2$O$_3$ can be related to the low acidity and low palladium penetration depth of the catalyst. The lower acidity of the support in combination with lower metal penetration depth might be limiting the beta hydride formation in the catalyst surface hence lowering the chances of hydrogen over reaction with the ethylene molecule formed. The ρ-Al$_2$O$_3$ behaves differently at higher temperatures, the lower acidity of the support might be preventing the interaction with the metal alumina support and the combination of higher temperature might be causing faster desorption of the hydrogen molecule from the catalyst surface, showing improved selectivity at higher temperatures [34–36].

The ability of Pd to react with hydrogen and form the β-hydride phase may play an important role in these catalysts. It was shown that the β-hydride phase favors the conversion of acetylene into ethane, with small Pd particles being more selective for ethylene formation. During reaction, palladium may get converted to β-PdH and these PdH decomposes and release hydrogen resulting in over hydrogenation of the alkene leading to alkane formation and carbonaceous or hydrocarbon species may get deposited on the surface of the catalyst. These deposits also favors the increased hydrogenation resulting in the conversion to ethane. It is known from literature that the presence of hydrogen residing the palladium sub surface will cause over hydrogenation of acetylene resulting in ethane formation [15]. In certain studies, ethylene TPD on different alumina species were done, the results show that high temperature ethylene desorption peaks were predominant in the catalyst with high surface area similar to Pd/γ-Al$_2$O$_3$ and Pd/δ-Al$_2$O$_3$ and high temperature desorption peaks were almost nil in Pd/α-Al$_2$O$_3$ [22]. The low temperature peaks in the ethylene desorption

studies were assigned to the π-bonded ethylene and the high temperature peaks are assigned to the di-σ bonded ethylene [37]. The low acidity of the Pd/α-Al$_2$O$_3$ might have led to predominant π-bonded ethylene intermediates, which dissociates easily from the catalyst site giving better selectivity. Studies have shown that the di-σ bonded ethylene formed on the catalyst site undergoes desorption slowly and it decomposes followed by reaction with the surface hydrogen to form ethylene and ethane [38]. Medium strength and high strength acid sites could give rise to green oil deposition during selective hydrogenation and these carbon deposits act as a hydrogen bridge for hydrogen spill over from the palladium to the support, facilitating ethylene hydrogenation to ethane.[39]. The palladium particle size analyzed using the TEM shows that Pd/α-Al$_2$O$_3$ catalyst has larger Pd particles compared to the other catalysts. Researches says that as the Pd particle size increases for the Pd on the surface, the selectivity increases [40]. The carbonaceous hydrocarbon deposits increase the mass transfer limitation on the catalyst surface limiting the dissociation mechanisms and increases the hydrogen concentration on the catalyst surface temporarily favoring over hydrogenation [41, 42].

Temperature programmed oxidation (TPO) of spent catalysts

To study the TPO, the spent catalysts were powdered and subjected to thermogravimetric analysis in air with a ramp rate of 10 °C/ min and up to 1000 °C. The mass spectrometer was connected to TGA machine and the mass fractions corresponding to CO$_2$ (44) and H$_2$O (18 and 17) were monitored to understand the weight loss was due to coking or heavy hydrocarbon formation on the catalysts during the reaction (Fig. 7).
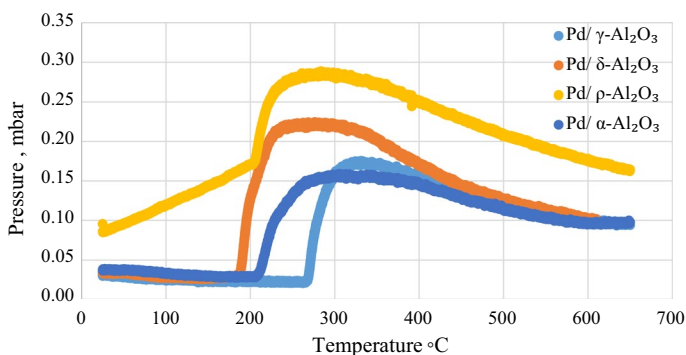
The weight loss in the thermogravimetric analysis for the spent catalyst could be due to the heavy hydrocarbon deposit on the catalyst. The mass spectroscopy data shows evolution of CO$_2$ (mass number 44) and evolution of mass fraction corresponding to H$_2$O (m/e 18). Figs. 8 and 9 indicate the evolution of CO$_2$ and H$_2$O for the different spent catalysts. Data show that combustion profiles are different and
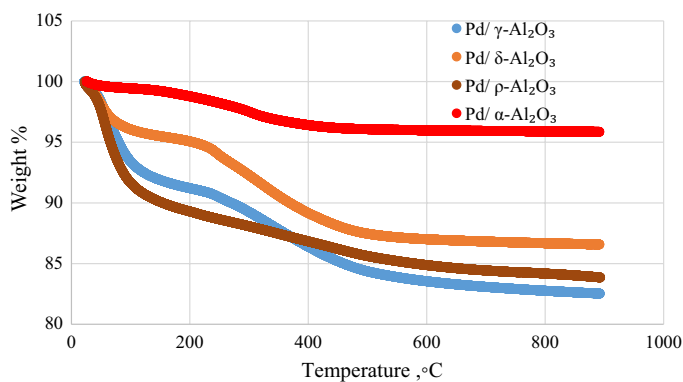
Fig. 7 TGA analysis spent catalysts done using SDT Q600 machine from 25 °C to 1000 °C in air at a ramp rate of 10 °C/min
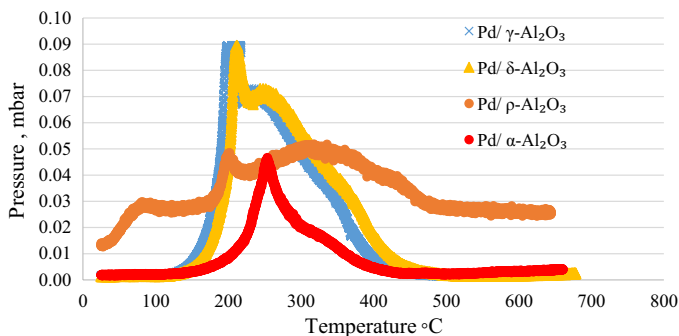
Fig. 8 Mass Spectra CO_2 (m/e 44)—evolved gas analysis for the spent catalysts (TGA coupled with mass spectroscopy)

Fig. 9 Mass Spectra H_2O (m/e 18)—evolved gas analysis for the spent catalysts (TGA coupled with mass spectroscopy)

Table 6 Spent catalyst weight loss from thermogravimetric analysis

Spent catalyst	% Weight loss at 200–600 °C
Pd/γ-Al$_2$O$_3$	8.9
Pd/ δ-Al$_2$O$_3$	8.7
Pd/ ρ-Al$_2$O$_3$	5.23
Pd/ α-Al$_2$O$_3$	3.25

hence the nature of carbonaceous species formed on the catalysts with different supports are different in nature.

The weight loss due to heavy component formation can be directly correlated with the catalyst activity and catalyst selectivity. Catalyst with highest activity and the lowest selectivity has attributed to higher heavy formation (Table 6). The catalysts Pd/γ-Al$_2$O$_3$ and Pd/δ-Al$_2$O$_3$ has the highest weight loss in the region 200 to 600 °C. The catalyst, Pd on α-Al$_2$O$_3$, with the highest selectivity showed the lowest

weight loss in the region 200 to 600 °C. The Pd/ρ-Al$_2$O$_3$ has lower acidity compared to the other supports contributing to low heavy formation compared to Pd /δ & Pd/γ-Al$_2$O$_3$ catalysts. The catalyst with high acidity has high carbon deposit and has lower ethylene selectivity as it favors over hydrogenation due to the hydrogen entrapped in the sub surface [43–46].

Conclusion

At temperatures below 100 °C, the catalyst prepared over α-Al$_2$O$_3$ observed to be more selective with the model feed. The better selectivity of the α-Al$_2$O$_3$ based catalyst could be due to the lower acidity of the support and lower penetration depth of the metal on the support. The beta hydride formation was found to be low at the operating temperature and hence better hydrogen dissociation could be achieved. The lower residence time for hydrogen on the support might have attributed to the higher selectivity. Higher temperature operation lowers the ethylene selectivity of the catalysts based on γ, δ and α-Al$_2$O$_3$, whereas the catalyst based on the ρ-Al$_2$O$_3$ support shows slightly better ethylene selectivity at higher temperature. The support acidity and palladium penetration depth of the catalyst plays vital role in the selectivity and conversion of the catalyst. The catalyst with the most dispersed active metal shows the highest conversion, here the γ-Al$_2$O$_3$ based catalyst has the most dispersed palladium, as it has the highest penetration depth. Thermogravimetric analysis of the spent samples were supporting the catalyst performance data, the highly active and less selective catalysts have higher weight loss at 200 to 600 °C. The mass spectroscopy data confirm the evolution of carbon dioxide at temperatures 200 to 600 °C, the higher weight loss was for the catalyst with low selectivity, the γ-Al$_2$O$_3$ and δ-Al$_2$O$_3$ based catalysts have higher weight loss at the mentioned temperature. The α-Al$_2$O$_3$ based catalyst has the lowest weight loss for the spent sample, which clearly supports the ethylene selectivity of the catalyst. The modern day bimetallic catalysts are based on the α-Al$_2$O$_3$ with Ag or Au added on to the catalyst for higher selectivity. The study done for acetylene hydrogenation in nitrogen environment gives information on the ideal behavior of the catalyst for selective hydrogenation of acetylene to ethylene.

Declarations

Conflict of interests The authors declare that they have no conflict of interests.

Consent to participate All authors participated in the creation of this manuscript.

Consent for publication All authors agree to publish this manuscript in the journal.

Availability of data and materials The authors confirm that the data and the findings mentioned in this study are available within the article and raw data and the derived data supporting the findings are available from the corresponding author on request.

References

1. Tiedtke DB, Bergmeister JJ, Cheung TP, Rhoades RA (2001) Progress in the development of E-Series catalyst technologies for the selective hydrogenation of acetylene in various hydrocarbon streams. Thai Olefins Ethylene Technology Forum
2. McCue AJ, Anderson JA (2015) Recent advances in selective acetylene hydrogenation using palladium containing catalysts. Front Chem Sci Eng 9:142–153. https://doi.org/10.1007/s11705-015-1516-4
3. Takht Ravanchi M, Fadaeerayeni S, Rahimi Fard M (2014) An egg-shell Pd-Ag/α-Al2O3 catalyst for tail-end acetylene selective hydrogenation. IJChE 11(1):42–54
4. Sivaraj CH, Contescue CR, Schwarz JA (1991) Effect of calcination temperature of alumina on the adsorption/impregnation of Pd(II) compounds. J Catal 132(2):422–431. https://doi.org/10.1016/0021-9517(91)90159-2
5. Hill MR, Bastow TJ, Celotto S, Hill AJ (2007) Integrated study of the calcination cycle from gibbsite to corundum. Chem Mater 19(11):2877–2883. https://doi.org/10.1021/cm070078f
6. Boumaza A, Favaro L, Lédion J et al (2009) Transition alumina phases induced by heat treatment of boehmite: An X-ray diffraction and infrared spectroscopy study. J Solid State Chem 182(5):1171–1176. https://doi.org/10.1016/j.jssc.2009.02.006
7. Takht Ravanchi M, Rahimi Fard M, Fadaeerayeeni S, Yaripour F (2015) Effect of calcination conditions on crystalline structure and pore size distribution for a mesoporous alumina. Chem Eng Commun 202(4):493–499. https://doi.org/10.1080/00986445.2013.850577
8. Chang PL, Yen FS, Cheng KC, Wen HL (2001) Examinations on critical and primary crystallite sizes during θ- to α-phase transformations of ultrafine alumina powders. Nano Lett 1(5):253–261. https://doi.org/10.1021/nl015501c
9. Iaponeide M, Macedo F, Aparecido Bertran C, Osawa CC (2007) Kinetic of the γ-to α-alumina transformation by quantitative X-ray diffraction. J Mater Sci 42:2830–2836. https://doi.org/10.1007/s10853-006-1364-1
10. Perander LM, Zujovic ZD, Groutso T, Hyland MM, Smith ME, O'Dell LA, Metson JB (2007) Characterization of metallurgical-grade aluminas and their precursors by 27Al NMR and XRD. Can J Chem 85(10):889–897. https://doi.org/10.1139/v07-106
11. Application note 134 https://www.micromeritics.com/Repository/Files/apnote134.pdf.
12. Gopinath R, Babu NS, Kumar JV, Lingaiah N, Prasad PS (2008) Influence of Pd precursor and method of preparation on hydrodechlorination activity of alumina supported palladium catalysts. Catal Lett 120:312–319. https://doi.org/10.1007/s10562-007-9287-2
13. Zhu Q, Gao J, Chen J, Wen L (2010) Selective hydrogenation of acetylene over egg-shell palladium nanocatalyst. J Nanosci Nanotechnol 10(9):5641–5647. https://doi.org/10.1166/jnn.2010.2472
14. Storozhenko PA, Aleshin AI, Douganyuk VF (2010) Selecting heat treatment conditions of alumina supports to improve the quality of selective hydrogenation palladium catalysts. Catal Ind 2:282–286. https://doi.org/10.1134/S207005041003013X
15. Khan NA, Shaikhutdinov S, Freund HJ (2006) Acetylene and ethylene hydrogenation on alumina supported Pd-Ag model catalysts. Catal Lett 108:159–164. https://doi.org/10.1007/s10562-006-0041-y

16. Ludwig W, Savara AA, Dostert K-H, Schauermann S (2011) Olefin hydrogenation on Pd model supported catalysts: new mechanistic insights. J Catal 284(2):148–156. https://doi.org/10.1016/j.jcat.2011.10.010

17. Paryjczak T, Rynkowski J (1984) Temperature-programmed reduction and temperature-programmed oxidation of nickel and copper-nickel catalysts with addition of palladium supported on alumina. React Kinet Mech Cat 24:187–191

18. Application note 120 "Temperature-Programmed Reduction Using the AutoChem" https://www.micromeritics.com/Repository/Files/appnote120.pdf

19. Sorbier L, Gay A-S, Fécant A, Moreaud M, Brodusch N (2013) Measurement of palladium crust thickness on catalysts by optical microscopy and image analysis. Microsc Microanal 19(2):293–299. https://doi.org/10.1017/S1431927612014316

20. Dehghani O, Rahimpour MR, Shariati A (2019) An experimental approach on industrial Pd-Ag supported α-Al$_2$O$_3$ catalyst used in acetylene hydrogenation process: mechanism, kinetic and catalyst decay. MDPI Process 27(3):136. https://doi.org/10.3390/pr7030136

21. Takht Ravanchi M, Fadaeerayeni S, Rahimi Fard M (2017) Acetylene selective hydrogenation: a technical review on catalytic aspects. Rev Chem Eng 34(2):215–237. https://doi.org/10.1515/REVCE-2016-0036

22. Komhom S, Mekasuwandumrong O, Praserthdam P, Panpranot J (2008) Improvement of Pd/Al2O3 catalyst performance in selective acetylene hydrogenation using mixed phases Al$_2$O$_3$ support. Catal Commun 10(1):86–91. https://doi.org/10.1016/j.catcom.2008.07.039

23. Taromi AA, Kaliaguine S (2017) Synthesis of ordered mesoporous γ-alumina: effects of calcination conditions and polymeric template concentration. Microporous Mesoporous Mater 248:179–191. https://doi.org/10.1016/j.micromeso.2017.04.040

24. Macêdo MIF, Bertran CA, Osawa CC (2007) Kinetics of the $\gamma \rightarrow \alpha$-alumina phase transformation by quantitative X-ray diffraction. J Mater Sci 42:2830–2836. https://doi.org/10.1007/s10853-006-1364-1

25. Ravanchi MT, Fadaeerayeni S, Fard MR (2016) The effect of calcination temperature on physicochemical properties of alumina as a support for acetylene selective hydrogenation catalyst. Res Chem Intermed 4(2):4797–4811. https://doi.org/10.1007/s11164-015-2320-y

26. Sung DM, Kim YH, Park ED, Yie JE (2010) Correlation between acidity and catalytic activity for the methanol dehydration over various aluminum oxides. Res Chem Intermed 36:653–660. https://doi.org/10.1007/s11164-010-0201-y

27. Standard Practice for Calculation of Pore Size Distributions of Catalysts and Catalyst Carriers from Nitrogen Desorption Isotherms, ASTM D4641-1. https://www.quantachrome.com/standards.html

28. Vaidya SD, Thakkar NV (2001) Effect of temperature, pH and ageing time on hydration of rho alumina by studying phase composition and surface properties of transition alumina obtained after thermal dehydration. Mater Lett 51(4):295–300. https://doi.org/10.1016/S0167-577X(01)00307-X

29. Bhogeswararao S, Srinivas D (2015) Catalytic conversion of furfural to industrial chemicals over supported Pt and Pd catalysts. J Catal 327:65–77. https://doi.org/10.1016/j.jcat.2015.04.018

30. Wongwaranom N, Mekasuwandumrong O, Praserthdam P, Panpranot P (2008) Performance of Pd catalysts supported on nanocrystalline α-Al2O3 and Ni-modified α-Al2O3 in selective hydrogenation of acetylene. Catal Today 131(1–4):553–558. https://doi.org/10.1016/j.cattod.2007.10.036

31. Duca D, Varga Z, La Manna G, Vidoczy T (2000) Hydrogenation of acetylene-ethylene mixtures on Pd catalysts: study of the surface mechanism by computational approaches, metal dispersion and activity of the catalyst. Theor Chem Acc 104:302–311. https://doi.org/10.1007/s002140000123

32. Komeilia S, Ravanchib MT, Taeb A (2015) The influence of alumina phases on the performance of the Pd–Ag/Al2O3catalyst in tail-end selective hydrogenation of acetylene. Appl Catal A 502:287–296. https://doi.org/10.1016/j.apcata.2015.06.013

33. Bos ANR, Westerterp KR (1993) Mechanism and kinetics of the selective hydrogenation of ethyne and ethane. Chem Eng Process 32(1):1–7. https://doi.org/10.1016/0255-2701(93)87001-B

34. Gislason J, Xia W, Sellers H (2002) Selective hydrogenation of acetylene in an ethylene rich flow: results of kinetic simulation. J Phys Chem 106(5):767–774. https://doi.org/10.1021/jp011238s

35. Battiston GC, Dalloro L, Tauszik GR (1982) Performance and aging of catalysts for the selective hydrogenation of acetylene: a micropilot-plant study. Appl Catal 2(1–2):1–17. https://doi.org/10.1016/0166-9834(82)80170-X

36. Ball MR, Rivera-Dones KR, Gilcher EB, Ausman SF, Hullfish CW, Lebrón EA, Dumesic JA (2020) AgPd and CuPd catalysts for selective hydrogenation of acetylene. ACS Catal 10(15):8567–8581. https://doi.org/10.1021/acscatal.0c01536

37. HeupMoon S-J (2011) Performance of Cu-promoted Pd catalysts prepared by adding Cu using a surface redox method in acetylene hydrogenation. Appl Catal A 401(1–2):12–19. https://doi.org/10.1016/j.apcata.2011.04.048

38. Zou S et al (2021) Grafting nanometer metal/oxide interface towards enhanced low-temperature acetylene semi-hydrogenation. Nat Commun 12:5570. https://doi.org/10.1038/s41467-021-25984-8

39. Feng J-T, Ma X-Y, Evans DG, Li D-Q (2011) Enhancement of metal dispersion and selective acetylene hydrogenation catalytic properties of a supported Pd catalyst. Ind Eng Chem Res 50(4):1947–1954. https://doi.org/10.1021/ie101508z

40. Ibhadon AO, Kansal SK (2018) The reduction of alkynes over Pd-based catalyst materials: a pathway to chemical synthesis. J Chem Eng Process Technol. https://doi.org/10.4172/2157-7048.1000376

41. Pradier CM, Mazina M, Berthier Y, Oudar J (1994) Hydrogenation of acetylene on palladium. J Mol Catal 89(1–2):20211–20220. https://doi.org/10.1016/0304-5102(93)E0323-9

42. Ravanchi MT, Sahebdelfar S, Komeili S (2018) Acetylene selective hydrogenation: a technical review on catalytic aspects. Rev Chem Eng 34(2):215–237. https://doi.org/10.1515/revce-2016-0036

43. Ravanchi MT, Sahebdelfar S, Fard MR, Fadaeerayeni S, Bigdeli P (2016) Pd-Ag/α-Al₂O₃ catalyst deactivation in acetylene selective hydrogenation. Chem Eng Process 39(2):301–310. https://doi.org/10.1002/ceat.201400526

44. Wang Z, Du W, Qian F, Tian L, Jiang D (2015) Improve acetylene hydrogenation selectivity using dynamic deactivation estimation. Hydrocarbon processing. Gulf Publishing Company, Houston

45. Kuhn M, Lucas M, Claus P (2015) Precise recognition of catalyst deactivation during acetylene hydrogenation studied with the advanced TEMKIN reactor. Catal Commun 72(5):170–173. https://doi.org/10.1016/j.catcom.2015.10.001

46. Samavatia M, Ebrahima HA, Dorjb Y (2018) Effect of the operating parameters on the simulation of acetylene hydrogenation reactor with catalyst deactivation. Appl Catal A 567:45–55. https://doi.org/10.1016/j.apcata.2018.06.038

Publisher's Note Springer Nature remains neutral with regard to jurisdictional claims in published maps and institutional affiliations.